2.2 PLAXIS 2D MODELING

An axisymmetric model is used to model the shaft. The soil and caliche are modeled using 15 node triangular elements. Linear elastic and Mohr-Coulomb constitutive models are used to model shaft and soil layers, respectively. Linear elastic constitutive model is used to model caliche in order to show its bending characteristic along with the monolith behavior of the deep foundation system. The linear elastic model, which is based on Hooke's law of linear elasticity, includes no failure criteria, and generally is not suitable for modeling soils. The linear elastic model is commonly used to model structural materials such as concrete. It is assumed that caliche behaves elastically like concrete. Hence, it is reasonable to use the linear elastic constitutive model for this material. The model requires two parameters; Young's modulus (E) and Poisson's ratio (ν). Elastic modulus of caliche can be estimated using empirical formula introduced by American Concrete Institute (2008) and National Cooperative Highway Research Program Report 496 (Tadros, 2003). Additionally, triaxial tests on core samples obtained from different project show a wide range for the elastic modulus of caliche ranging between 300,000-700,000 ksf. Average values are used to estimate the elastic modulus of gravel and clay based on the studies by Das (2010), Bowles (1988) and Coduto (2001). Least squares regression method is used to minimize the difference between calculated and measured results. The final PLAXIS model input parameters after the regression is shown in Table 1.

Table 1. Back analysis model soil, caliche and concrete parameters

PLAXIS Parameters		Concrete	Caliche	Sand & gravel	Stiff Clay
Drainage		Drained	Drained	Drained	Drained
γ_{unsat}	[klb/ft³]	0.15	0.16	0.12	0.13
γ_{sat}	[klb/ft³]	0.15	0.16	0.13	0.13
E_{ref}	[klb/ft²]	750,000	600,000	3,000	1,000
ν	[-]	0.15	0.30	0.30	0.40
c_{ref}	[klb/ft²]	-	-	0.10	0.20
φ	[°]	-	-	45.0	30.0
Ψ	[°]	-	-	10.0	0.0
E_{inc}	[klb/ft²/ft]	-	-	0.0	12.0
y_{ref}	[ft]	-	-	0.0	-16.0
$c_{increment}$	[klb/ft²/ft]	-	-	0.0	0.0
$T_{str.}$	[klb/ft²]	-	-	0.0	0.0
$R_{inter.}$	[-]	1	1.0	1.0	0.80

2.3 ANALYSIS AND RESULTS

The PLAXIS model is calibrated for upward and downward loading of the shaft separately. The results of PLAXIS analysis are presented in FIG. 3. The analytical results show good compatibility with the o-cell load test results.

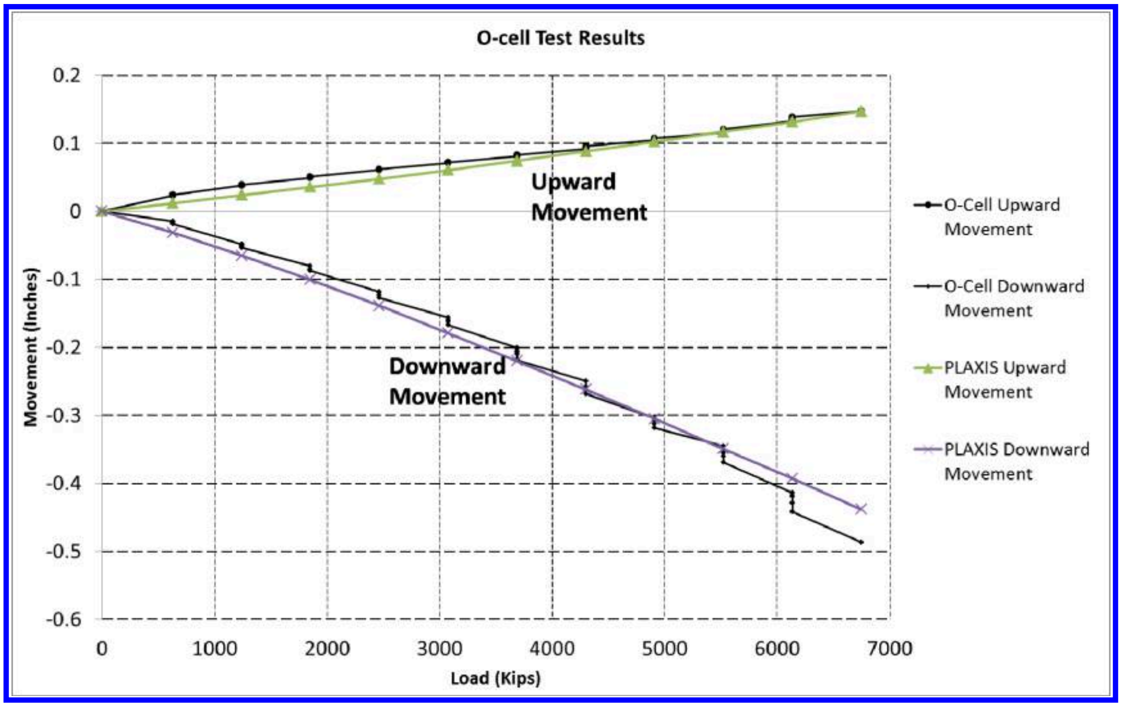

FIG. 3. PLAXIS vs. field test results

Interface elements in PLAXIS can help understanding the behavior of shaft-soil system particularly the slippage between the shaft and soil layers. After calibrating the model, the shear stress and slippage values at the interface is individualized for each soil layer and studied in detail. The results from PLAXIS model show limited slippage between the shaft and the soil layers as shown in FIG. 4. The ultimate skin resistance in the shaft is fully mobilized when the slippage between the soil and the shaft is about 0.2-0.3 inches. The results show that the maximum experienced slippage between the shaft and soil layers is less than what is required to generate the ultimate skin resistance values. Additionally, FIG. 4 shows a roughly elastic behavior in the soil layers due to relatively small slippage in the presence of caliche layers. As shown in FIG. 5, the slippage decreases even more at the interface between the shaft and caliche layers, signifying the monolithic behavior of shaft-caliche system.

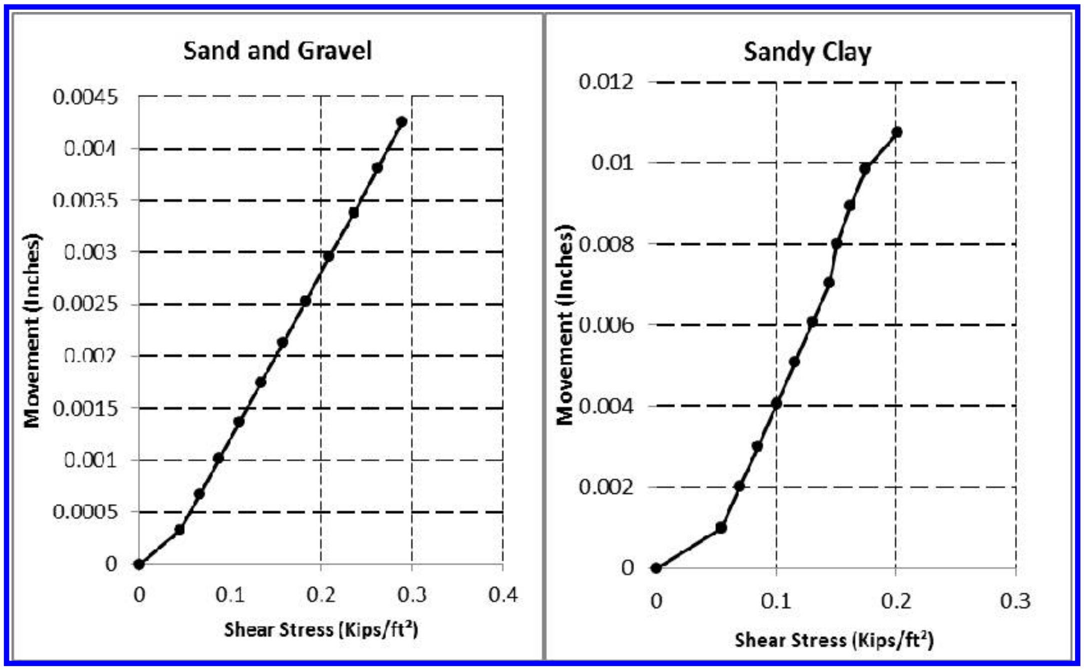

FIG. 4. Shear stress vs displacement

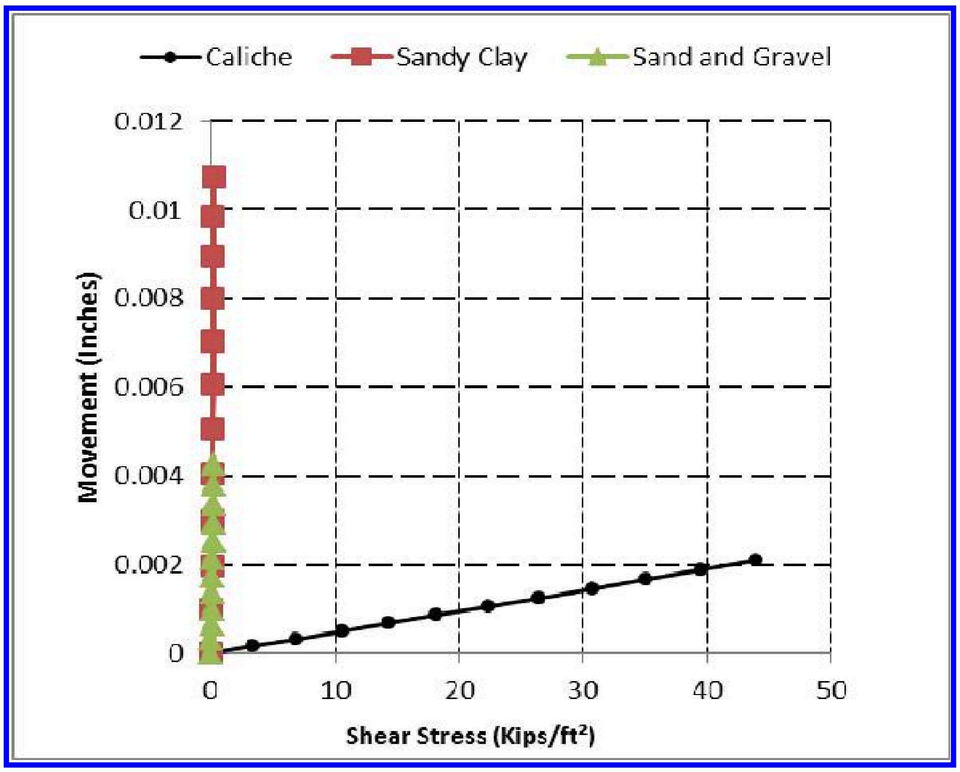

FIG. 5. Comparison of caliche, sand and gravel and sandy clay

3 CONCLUSIONS

The bonding between caliche layers and the shaft is very strong and prevents slippage. Thus, traditional design methodologies based on ultimate skin friction may not applicable to drilled shafts analysis and design in caliche. The slippage values for sand & gravel and sandy clay show that the soil layers are not mobilized enough to generate ultimate skin resistance. Additionally, the slippage value drops even more at the interface between the shaft and caliche layers, indicating, that the caliche layers and the shaft behave monolithically. The research suggests that caliche layers reduce the slippage values by holding on to the shaft resulting in an elastic system. Further investigations need to be performed toward analysis of osterberg test. The monolith behavior of drilled shafts in caliche may change the current method used to interpret o-cell test results.

4 REFERENCES

ACI Committee 318. (2008). *Building code requirements for structural concrete (ACI 318-08) and commentary* American Concrete Institute, 2008.

Bowles, J. E. (1988). *Foundation analysis and design*

Cibor, J. M. (1983). Geotechnical considerations of las vegas valley. Paper presented at the *Geological Environmental and Soil Properties,* 351-373.

Coduto, D. P. (2001). *Foundation design: Principles and practices* Prentice Hall Upper Saddle River.

Das, B. (2010). *Principles of foundation engineering* Cengage Learning.

Standard test methods for deep foundations under static axial compressive load. (2013). *American society for testing and materials, annual book of ASTM standards* (04.08th ed.,)

Tadros, M. K. (2003). *Prestress losses in pretensioned high-strength concrete bridge girders* Transportation Research Board.

Numerical Simulation of a Drilled Shaft in an MSE Wall under Cyclic Loading

Md. Saidur Rahman[1], Jie Huang[2]* M.ASCE, P.E., and Sazzad Bin-Shafique[3], P.E.

[1] Geotechnical engineer, GTS Technologies, Inc, 441 Friendship Road, Harrisburg, PA, 17111 (former graduate student of University of Texas at San Antonio)
[2]*corresponding author, assistant professor, Department of Civil and Environmental Engineering, University of Texas at San Antonio, One UTSA Circle, San Antonio, TX, 78249, Tel: (210) 458-7908; Fax: (210) 458-6475; jie.huang@utsa.edu
[3] Associate professor, University of Texas at San Antonio, One UTSA Circle, San Antonio, TX, 78249

ABSTRACT: A numerical simulation was conducted using FLAC3D to investigate the interaction between the drilled shaft and the MSE wall under lateral cyclic loading that are often encountered from bridges, traffic signs, and sound walls. The drilled shaft was built within the reinforced zone of an MSE wall and loaded toward the MSE wall under force-control mode. An elastoplastic constitutive model, able to consider shear and compression hardening, was selected for the backfill material. The MSE wall facing was simulated by discrete blocks which interacted with each other by friction. The selected constitutive model was calibrated by triaxial test data. Thereafter, the numerical modeling was conducted to simulate a published full-scale field study on the interaction between the drilled shaft and the MSE wall. It was found the developed numerical model can well represent the loading-unloading behavior of the drilled shaft and the MSE wall. As the drilled shaft was laterally loaded to a large deflection, only small percentage of the deflection could recover when the load was removed. As to the MSE wall, nearly all the deformations induced were not recoverable. It was suggested the numerical model be further improved by accounting for the separation between the MSE wall facing blocks.

INTRODUCTION

In recent years, the use of laterally loaded drilled shafts, which are built in a mechanically stabilized earth (MSE) wall, has become more popular due to the space constraint (Berg et al. 2009; Pierson et al. 2011; Huang et al. 2013). So far, there is no design method available to consider the interaction between the MSE wall and the drilled shaft. Therefore, the MSE wall and drilled shaft are design independently (Pierson 2007). Such design simplification has resulted in overdesigned drilled shafts by ignoring the support from the MSE wall as well as underdesigned MSE walls due to neglecting the additional pressure from drilled shafts. Some distresses of MSE walls have been observed (Berg et al. 2009).

Only a few studies have been completed to study the interaction between the MSE wall and drilled shaft. Pierson et al. (2008) performed a full-scale experimental study to evaluated the support that an MSE can provide for a laterally loaded shaft and a group of shafts. The study was conducted within a 43 m long MSE wall with geogrid reinforcement. The wall was divided into multiple test sections with one drilled shaft or multiple drilled shafts constructed within each test section (Pierson 2007; Pierson et al. 2008; Pierson et al. 2011). The shaft(s) was laterally loaded until large deflection (i.e., >100 mm). It was found that the MSE wall could provide significant lateral support for the drilled shaft and the magnitude of the support depended on the embedment length of the drilled shaft in the MSE wall and the distance between the drilled shaft and the MSE wall. A numerical simulation has been carried out to investigate the influence of various factors on the interactions between the MSE wall and drilled shafts (Huang et al. 2011; Huang et al. 2013). Texas Department of Transportation (TxDOT) recently sponsored a study to assess the interaction between drilled shaft and an MSE wall that used metallic reinforcement.

All the completed studies are focused on monotonic loading conditions but the drilled shafts are often subjected to loading-unloading cycles such as wind load. This paper presents a numerical simulation of the drilled shaft within an MSE wall under cyclic loading condition.

PROTOTYPE OF THE NUMERICAL MODEL

One of the test sections, including a 0.9 m diameter drilled shaft located at 3.6 m from the MSE wall, was used as the basis of this study and shown in Figure 1.

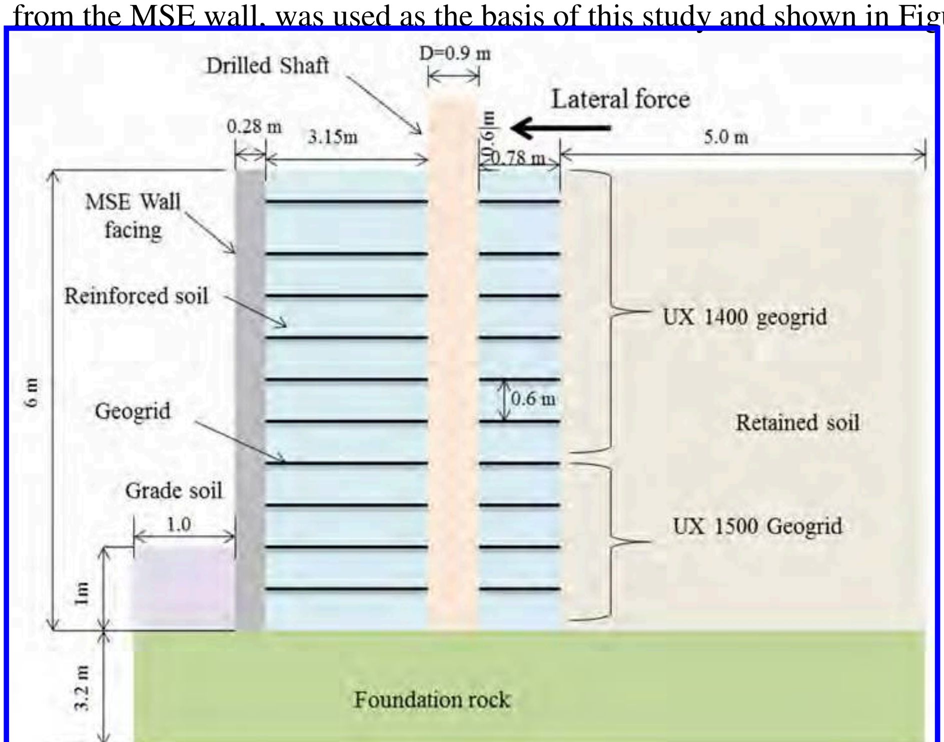

FIG. 1. Cross-section of the selected the test section.

The MSE wall was 6 m tall and had UX 1500 (Geogrid A) and UX 1400 (Geogrid B) geogrid as reinforcement. The poorly graded gravel (GP) was used a backfill material which had a maximum particle size of 20 mm. The D_{10}, D_{30} and D_{60} are 3, 6, and 15 mm respectively. Mesa blocks with dimensions of 0.45×0.28×0.2 m^3 (long × width × height) were used as facing units. The MSE wall and drilled shaft were situated on top of weathered limestone. A concentrated lateral force was at 0.6 m above the top of the MSE wall. The deflection, applied load, and earth pressure were monitored by LVDT, earth pressure cells, load cells and photogrammetry. The detailed information about the instrumentation and data acquisition can be found from (Pierson 2007) and (Pierson et al. 2008).

NUMERICAL MODEL

The three-dimensional (3D) finite difference software, FLAC3D, is utilized in this study for the numerical analysis.

Constitutive Models

Three different constitutive models are used for backfill material, grade soil, retained soil, foundation soil, MSE wall facing, drilled shaft, and geogrid materials. The material properties are presented in Table 1. The linearly elastic perfectly plastic model with Mohr-Coulomb model was used from retained soil, and grade soil. Elastic model was used for MSE wall facing, drilled shaft, foundation rock and geogrid. The backfill material was simulated by so-called the Cap-Yield model in FLAC3D (Itasca 2009). The Cap-Yield model is comprised of two yield surface, namely, isotropic compression yielding and shear yielding. The shear yield surface is a rotary surface symmetric to the mean stress axis, which is formulated in Eq. 1, while the compression yield surface is a curved surface perpendicularly to the mean stress axis, which is formulated in Eq. 2.

$$f^{sh} = \mathrm{M}p' - \mathrm{q} \tag{1}$$

$$f^{cp} = \frac{q^2}{\alpha^2} + p'^2 - p_c^2 \tag{2}$$

where α is a dimensionless parameter, which defines the shape of the elliptical cap yield surface (α=1, spherical; α<1, ellipsoidal); p_c is the cap pressure which defines the size of the compression yielding surface; $\delta = (3+\sin\phi_m)/(3-\sin\phi_m)$; $M = 6\sin\phi_m/(3-\sin\phi_m)$; $p' = (\sigma_1'+\sigma_2'+\sigma_3')/3$; $q = (\sigma_1'+(\delta-1)\,\sigma_2'-\delta\sigma_3')$. ϕ_m is the mobilized friction angle which is a function of the total plastic shear strain. The relationship between plastic shear strain, γ^p and mobilized friction angle, ϕ_m is formulated in Eq. 3.

$$\gamma^p = \frac{p_{ref}}{G_{ref}^e}\frac{\sin\phi_f}{R_f}\left[\frac{1}{1-\dfrac{\sin\phi_m}{\sin\phi_f}R_f} - 1\right] \tag{3}$$

where p_{ref} is the reference mean stress; ϕ_f is the ultimate friction angle; R_f is a constant which is less than 1; and G^e_{ref} is the stress modulus at the reference pressure, p_{ref}. G^e_{ref} is determined from K_{ref} which can be described by a hyperbolic law according to traixial test data of Pierson (2007) and back analysis of Huang et al. (2013). The determined formula of K_{ref} is shown in Eq. 4.

$$K_{ref} = 45(\frac{\sigma_3}{P_a})^{0.65} \tag{4}$$

The compression yielding follows the associated flow, but the shear yielding follows the associated flow as formulated in Eq. 5.

$$g = \sigma_1^{'} - \sigma_3^{'} \tag{5}$$

where σ_1 and σ_3 are major and minor principal stresses, respectively.

The compression hardening behavior of the soil is considered as the expansion of the cap yielding surface as formulated in Eq. 6.

$$p_c = p_{ref}[\frac{1}{2}\frac{1+R}{R}\frac{K_{ref}}{p_{ref}}\varepsilon_v^p]^2 \tag{6}$$

where ε_v^p is the plastic volumetric strain; R, a constant, is the ratio of volumetric plastic strain to volumetric elastic strain.

Table 1. Models and Material Properties (Modified after (Huang et al. 2013)).

Materials	Constitutive models	Material properties
Drilled shaft	Elastic	E = 30 GPa, υ = 0.3, γ = 25 kN/m^3
Facing blocks	Elastic	E = 2 GPa, υ = 0.25, γ = 15 kN/m^3
Backfill materials	Cap-Yield model	α = 1, υ = 0.2, γ = 18 kN/m^3, ϕ_f= 48°, R_f= 0.9, R = 0.6, $p_{ref} = \gamma H$
Retained soil	Linearly-elastic perfectly-plastic	E = 30 GPa, υ =0.3, γ = 17.5 kN/m^3, ϕ = 35°, c = 0 kPa
Grade soil	Linearly-elastic perfectly-plastic	E = 30 GPa, υ =0.3, γ = 17.5 kN/m^3, ϕ = 40°, c = 0 kPa
Foundation rock	Elastic	E = 30 GPa, υ = 0.3, γ = 17 kN/m^3
Geogrid A	Elastic	J_{MD} = 1900 kN/m, J_{CMD} = 190 kN/m
Geogrid B	Elastic	J_{MD} = 1040 kN/m, J_{CMD} = 104 kN/m

Note: E = elastic modulus; υ = Poisson's ratio; ϕ = friction angle; c = cohesion; γ = unit weight; J_{MD} and J_{CMD} = tensile stiffness in machine and cross machine directions.

Interface Models

The contacts between dissimilar materials were represented by interfaces. The interface properties are provided in Table 2. All of the interfaces were modelled as

Mohr-Coulomb sliders which are a linearly-elastic perfectly-plastic spring with the Mohr-Coulomb failure criterion. The properties of the interfaces were determined based on test data, such as Pierson (2007) and Pierson et al. (2008), or based on published data, such as Ling et al. (2004) and Huang et al. (2009). More details discussion about the interface properties should be referred to Huang et al. (2013).

Table 2. Interface properties.

Interfaces		Interface properties
MSE wall facing blocks	Horizontal	ϕ_i = 57°, c_i = 46 kPa, k_s = 40 MN/m/m, k_n = 40 MN/m/m
	Vertical	ϕ_i = 19.5°, c_i = 0.5 kPa, k_s = 40 MN/m/m, k_n = 40 MN/m/m
MSE wall facing blocks and backfill soil		ϕ_i = 44°, c_i = 0 MPa, k_s = 40 MN/m/m, k_n = 40 MN/m/m
Drilled shaft and backfill soil		ϕ_i = 41°, k_s = 15.38 MN/m/m, k_n = 33.33 MN/m/m
Geogrid A and backfill soil		ϕ_i = 48°, c_i = 0, k_s = 95,000 kN/m/m
Geogrid B and backfill soil		ϕ_i = 48°, c_i = 0, k_s = 52,000 kN/m/m

Note: ϕ_i = the interface friction angle; c_i = interface cohesion; ks = interface shear stiffness; and kn = interface normal stiffness.

Modeling Procedure

The numerical simulation started with validation of the Cap-Yield model. The published triaxial test data were used for this purpose. Thereafter, the numerical simulation of the drilled shaft and MSE wall was conducted. The three-dimensional (3D) FLAC3D model is presented in Fig. 2.

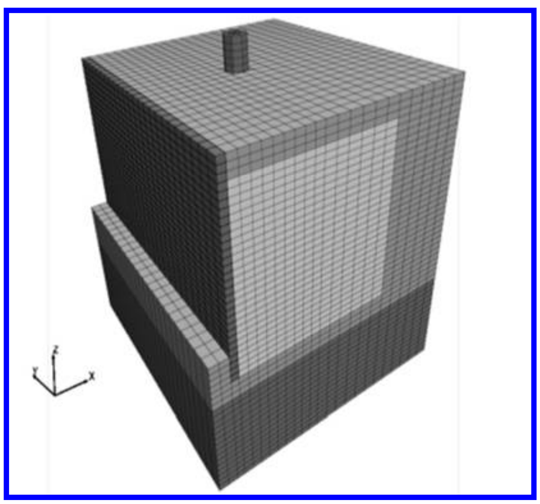

FIG. 2. FLAC3D model.

This modeling was implemented sequentially in three major steps: initiation of the stress field of the foundation, the construction of the MSE wall by three lifts, and testing the drilled shaft. In the construction, the 6 m MSE wall was constructed by 3 lifts of equal thickness (i.e., 2 m of backfilling for each lift). The compaction of the backfill was considered by initializing additional horizontal stress according to Filz and Duncan (1996) and Ehrlich et al. (2012). For the drilled shaft testing, the drilled shaft was laterally loaded toward the MSE wall and then unloaded following the test procedure of Pierson (2007).

RESULTS AND DISCUSSIONS

Verification of Cap-Yield Model by Triaxial Data

Three sets of triaxial tests were conducted by (Pierson 2007), which were under confining stress of 35, 70, and 140 kPa respectively. The Cap-Yield model was employed to simulate the triaxial tests. The obtained stress-strain curves were compared with these from triaxial tests as shown in Fig. 3. There is a good agreement between numerical results and test data as there is limited variation between the curves. In simulation, a few loading-unloading cycles were applied to examine whether the Cap-Yield model can well represent the hysteresis effect of the soil. Obviously, selected model (i.e., Cap-Yield model) can well represent the stress-strain behavior of the loading-unloading cycles.

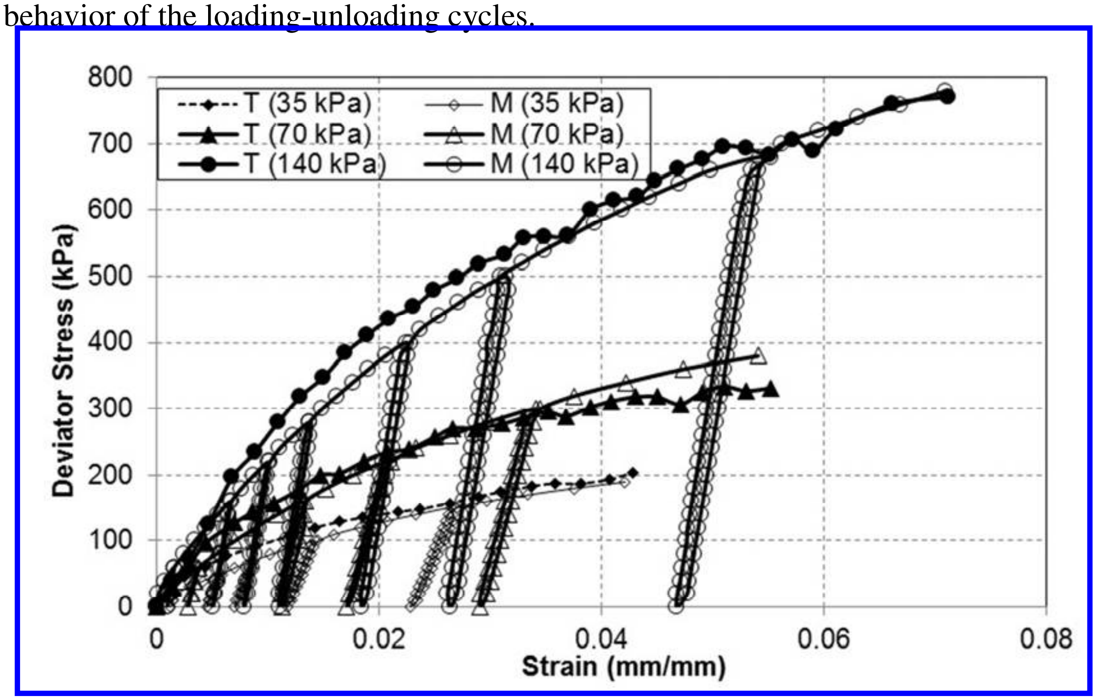

FIG. 3. Stress vs. deviator stress for triaxial tests.

Drilled Shaft Deflection

For the test section, the drilled shaft was loaded and then unloaded once. The test scheme was replicated except the loading modes. In the field test, the drilled shaft